# Electromagnetic Crystals for Surface Plasmon Polaritons and the Extraction of Light from Emissive Devices

W. L. Barnes

***Abstract*— Periodically textured metallic films are discussed as a method of extracting light from thin-film emissive devices. The proposed scheme involves coupling the emitters to a surface plasmon polariton mode of the structure and producing useful radiation by scattering this mode off periodic microstructure. The concepts involved are developed and the details associated with several specific candidate structures explored. The potential of these structures to enhance the emissive process is assessed, and possible problems, especially loss in the metal, are discussed.**

***Index Terms*—Light-emitting diodes, periodic structures, spontaneous emission, surface waves.**

## I. Introduction

GENERATING light has been an important part of science and technology for millennia. Today it is still the subject of intensive activity. In 1997, an estimated $10^{17}$ J were consumed by the United Kingdom alone in generating space light at a cost of £3bn [1]. Solid-state optical sources, especially the light-emitting diode (LED), are now being considered for applications such as space lighting. Producing light in this way typically involves the creation of an exciton via the injection of charge carriers, electrons, and holes into a semiconducting material where they may recombine radiatively, so producing light. Bearing in mind the figures concerning energy consumption above, the question of efficiency of the LED is an important one, to which there are many facets: injection of carriers, competition between radiative and nonradiative recombination, etc. This paper is concerned with the efficiency with which light may usefully be extracted from the device via the radiative recombination process.

The LED usually comprises a thin film of emissive material. Light is generated within the film in the recombination zone and must then leave the film if it is to provide useful output. A considerable fraction of the light is usually trapped within the film, limiting the efficiency of the device. The scheme explored in this work is one way in which this problem might be overcome.

## II. The Problem of Getting Light Out

The nature of the problem is easily discussed with the aid of a schematic diagram of a generic light-emitting diode (Fig. 1).

Manuscript received June 8, 1999; revised July 9, 1999. This work was supported by EPSRC and the Leverhulme Trust.

The author is with the School of Physics, University of Exeter, Exeter EX4 4QL UK (e-mail: w.l.barnes@ex.ac.uk).

Publisher Item Identifier S 0733-8724(99)08820-9.

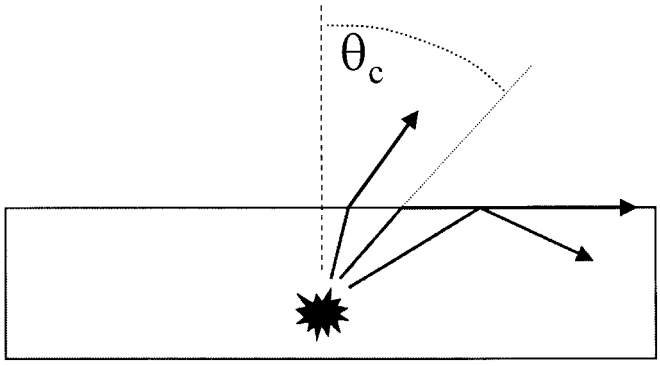


Fig. 1. The problem of extracting light from a thin film of material whose permittivity $\varepsilon$ is higher than that of the surrounding media is depicted. Only light within a cone defined by the critical angle $\Theta_c$ may escape.

Only emission into angles— $-\theta_c < \theta < \theta_c$, where $\theta_c$ is the critical angle—results in emission from the structure, the rest being trapped as guided light by total internal reflection. An approximate expression for the fraction of light that escapes is $1/2n^2$, $n$ being the refractive index of the emissive material [2]. For LED's based on polymeric materials having a refractive index $n = 2$, only approximately 13% of emission results in useful radiation; for a semiconductor such as GaAs, the problem is even more severe since the index is even higher, $n = 3.5$, so that only approximately 5% of the emission is useful. The remainder of the power is trapped by the multilayer structure of the LED and either is absorbed by the materials present or emerges from the edge of the device where recovering it as useful radiation may prove difficult. A more sophisticated model that takes proper account of the electromagnetic modes of the structure and the dipole nature of the emitting sources differs in the detail but reaches the same basic conclusion: a significant fraction of the light is trapped by the structure, unable to emerge as useful radiation [3], [4].

Several ways of overcoming this limitation have been investigated, principal of which is enclosing the emissive layer inside an optical microcavity [5]–[7]. Examining Fig. 1, we see that our structure is already a planar microcavity, albeit with relatively weak mirrors: the interface between the material in which the emitter is embedded and the surrounding media. Increasing the $Q$ of our cavity by making these mirrors so that they have high reflectivity for all angles of incidence (not just those above the critical angle) changes the nature of the problem. Previously, the light that was directly radiated could be so over a range of angles, i.e., there was a continuum

of radiative modes. Increasing the reflectivity of the mirrors results in only discrete modes of the microcavity's being allowed. If we make our microcavity so thin that it is only able to support the fundamental mode (for which the cavity thickness is approximately $\lambda/2$), then the fraction of power emitted into this mode will have been optimized, the number of alternative routes by which energy may be lost from the emitter (surface modes, modes of the mirrors, and absorption) having been minimized [4], [8].

Calculations indicate that using such an approach, up to 32% may be coupled to useful radiation compared to the $1/2n^2$ value of 12.5% for the polymeric emissive layer considered [3]. The microcavity clearly provides a beneficial effect in this case.

A subtle variation on this theme occurs if the emissive sources can be re-excited by absorbing light trapped within the cavity. When such re-excited emitters radiate, they have a probability of doing so into the mode that produces useful radiation. Re-emission that is trapped may go through the process again, and so on. If absorption within the microcavity, other than by unexcited emitters, is low, this process, known as photon recycling, may be used to increase the overall radiative efficiency of the device [9].

Using this approach, the group at IMEC, Leuven, Belgium, recently demonstrated an external quantum efficiency of 22% for a planar microcavity device [10]. The question that concerns us here is, how can one do better? In essence, there are two alternatives.

1) Block emission into those modes that do not contribute to usefully radiated output. This is one area in which electromagnetic crystals may be used. By introducing periodic microstructure in the plane of the microcavity, we hope to block the propagation of the wasteful guided modes by introducing a bandgap. In the frequency range spanned by the bandgap, the guided modes will no longer be supported by the structure. If the emission frequency of the emitters lies in this gap, then emission into the guided mode may no longer take place. This should result in a greater proportion of the power's being coupled to the useful, radiative mode.
2) Rather than blocking the guided modes, one may try instead to recover them. This may be done using a similar method to that deployed above, by using periodic microstructure. In this case, however, the periodicity is chosen such that the guide mode is scattered out as radiation, rather than being back-scattered by Bragg scattering off the microstructure to produce a bandgap. This phenomenon has been widely observed [11] but has only relatively recently been applied to the problem of extracting light from an LED [12]. Indeed, the IMEC group has very recently used microstructure to increase the extraction efficiency to 31% from the 22% obtained for the planar device [10].

One aspect of microcavities that we have not discussed so far is the effect the microcavity has on the decay rate. Placing an emitter in a microcavity not only changes the modes it may couple to; the fields reflected back to the dipole site by the structure also drive the emission process. If these reflected fields are in phase with the source term, then emission is enhanced and the decay rate increased; if they are out of phase, then emission is inhibited and the rate is reduced [13]. From the perspective of efficiency, this is only important if nonradiative decay of the emissive species is significant. If such is the case, then increasing the rate of spontaneous emission may also increase the efficiency since radiative decay will compete more effectively with nonradiative decay. Ideally, one would like to combine a significant increase in the rate of spontaneous emission together with a mechanism for ensuring efficient extraction of this energy. For this reason, blocking guided modes by introducing a bandgap seems less favorable than using such modes in the emission process.

The process just mentioned uses a guided wave as an intermediate step in the generation of light from a thin film of emissive material; it may offer an efficient route for extracting light [14]. In the next section, the advantages and problems associated with the approach are outlined. Subsequent sections examine these issues in more detail with particular reference to four specific structures. In all four cases, the guided mode selected as the intermediary is a surface plasmon polariton (SPP) mode. The reasons for this choice are elaborated by drawing on the background physics of these modes.

## III. The Concept

The essence of the proposed method for extracting light is this. The emissive species couples to a guided mode of the structure. The guided mode then scatters off some periodic aspect of the structure to produce useful radiation. Already it is clear that we are discussing a nonplanar structure. The reasons why this approach may be advantageous, and the questions that need to be addressed, are discussed in this paper. It is useful to summarize them at this stage.

The *advantages* are the following.

- Guided modes may have significantly enhanced electric fields associated with them. This leads to very effective coupling of the emitter to the mode and an associated increase in the rate of spontaneous emission [15].
- The emission process is now separated from the production of the radiated energy by the intermediate step, the guided mode. This should allow greater control over the emitted radiation, e.g., the spatial distribution of the radiated power.

The principal *questions* that need addressing are the following.

- Can the dissipative loss that is associated with modes that propagate at least in part in metallic media be circumvented? The surface plasmon polariton modes proposed here are guided by the interface between a metal and a dielectric, so that this question is of key importance to us.
- Can effective control over the second stage of the process, coupling the intermediate mode to useful radiation, be achieved with a structure that still offers significant advantages for the first stage, i.e., coupling of the emitter to the SPP mode?

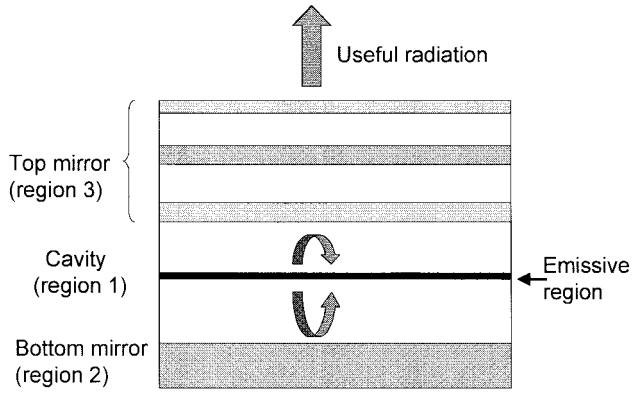


Fig. 2. Schematic of the microcavity. The emitters are embedded in medium 1. The field produced by the emitters is reflected by the structures (mirrors) above, region 3, and below, region 2. The reflected fields modify the emission process.

- What are the best structures for this scheme? How easy will they be to fabricate?

## IV. Where Does the Rest of the Energy Go?

We mentioned above that a microcavity could increase the fraction of the emitted power that results in radiation's leaving the structure. However, a significant fraction is still not producing useful radiation. What happens to this power? It is presumably dissipated into other modes of the structure, but what is the nature of these modes? Although this subject has been addressed by many authors [3], [8], [15], [16], it is essential that we have a clear view of the answer to this question if we are to try and find ways of increasing the fraction of power that is radiated. It is therefore worth examining in some detail the modes associated with typical microcavity light-emitting structures. The typical microcavity LED comprises two mirrors, which are sandwiched between the emissive layer (Fig. 2). The mirrors may be either distributed Bragg reflectors (DBR's) based on multilayer dielectric stacks or metals. Metals are often used as mirrors because they can also serve as an electrode.

We are concerned here with where the power emitted by sources within such structures is dissipated. To investigate this, and to help build an intuitive picture of the processes involved, a theoretical model is of considerable use. Suitable models are well established, so that only the briefest description will be given here [17]. We will concentrate on using such models to build an understanding of the modes into which power may be lost in the structures of interest to us.

## V. The Model

A well-proven model applicable to the present situation uses an entirely classical formalism. The emitter is considered to be a *forced, damped, electric dipole oscillator* located in a planar multilayer structure (Fig. 2). It is *electric dipole* since this is the nature of many transitions that give rise to optical radiation. It is *damped* because the oscillator loses energy to its surroundings by coupling to the available modes of the surrounding structure. It is *forced* because fields produced by the dipole are reflected by the surrounding structure back to the dipole site. These reflected fields act to drive the oscillator. If they are in phase, emission is enhanced and the decay rate increased. If they are out of phase, emission is inhibited and the decay rate reduced.

The decay rate of the oscillator is given by the rate at which the dipole moment $\boldsymbol{p}$ does work on the field $\boldsymbol{E}$ that it produces. This rate$b$ is given by

$$b = -\frac{\omega}{2}\mathrm{Im}(\boldsymbol{p}^*.\boldsymbol{E}) \tag{1}$$

where $\omega$ is the angular frequency of the oscillation. The field $\boldsymbol{E}$ comprises two contributions: a component due directly to the dipole moment and a component due to fields reflected back to the dipole site. To find the decay rate in a given situation, we need to find the value of the reflected field. The calculation comprises several stages.

- Expand the dipole field as a sum of plane waves, each component of which is characterized by a wavevector in the plane of the microcavity, the in-plane wavevector.
- Calculate the field reflected by the multilayer structure above and the structure below the dipole source. The reason for expanding the dipole field in terms of plane waves characterized by different in-plane wavevectors is now clear; the reflection coefficient for such waves is easily computed using Fresnel's reflection formulas [18].
- Calculate the reflected field at the site of the dipole, integrating over all the contributions from different in-plane wavevectors and taking account of retardation, i.e., the phase change in going from the dipole to the interface and back.
- Divide the resulting expression for the decay rate [(1)] by the value of the decay rate for the source embedded in the same material, but infinite in extent, i.e., no reflections $b_0$. The result for any dipole orientation may be considered as a combination of dipole moments perpendicular $(\perp)$ and parallel $(||)$ to the dipole the plane of the structure. We thus find, for the normalized decay rate

$$\frac{b_{\perp,||}}{b_0} = 1 - q + q\int_0^\infty I_{\perp,||}(u)\,du \tag{2}$$

where $q$ is the radiative quantum efficiency of the emitter in the material in which the dipole resides. The integrands $I_\perp$ and $I_{||}$ are given by (3) and (4), shown at the bottom of the next page.

Several parameters need explaining here. The variable of integration $u$ is the component of the wavevector (of the dipole field) in the plane of the interface, normalized with respect to the far-field wavevector $k_1$ of the dipole radiation field in medium 1. The parameter $l_1$ is given by $l_1 = -i(1-u^2)^{1/2}$ and is related to the component of the wavevector perpendicular to the interface. The coefficients $r^p_{1,j}$ and $r^s_{1,j}$ are the Fresnel reflection coefficients for, respectively, $P$ and $S$ polarized light at the interface between the cavity medium and the region $j$ (see Fig. 2) evaluated as a function of $u$. (The reflection coefficients at these interfaces take account of all the media and interfaces that compose the semi-infinite regions beyond the interface immediately adjacent to the

cavity [19].) Since $u$ may range over all positive values between zero and $\infty$, the reflection coefficients have to be calculated for both real and complex angles of incidence. These correspond to incident waves that are propagating and evanescent, respectively. The phase angle $\beta_{1,j}$ is the phase due to retardation, i.e., the phase change incurred in the round trip from the emitter, to the $1, j$ interface, and back.

For many emissive systems, the dipole moment associated with the transition rotates rapidly compared to the emission lifetime. In this case, the dipole moment samples all directions equally, and the lifetime is then given by $b_{\text{iso}}/b_o$

$$\frac{b_{\text{iso}}}{b_o} = \frac{2}{3}\frac{b_{\|}}{b_o} + \frac{1}{3}\frac{b_{\perp}}{b_o} \tag{5}$$

and is referred to as the isotropic case. The results of this model, (2)–(5), can be used in several interesting ways.

- It is clear that they can be used to compute the decay rate. It is perhaps worth noting at this stage that the modes supported by a given structure are dictated by the permittivity and thickness of the layers that it comprises. The decay rate depends on the strength of the coupling to these different modes that the source experiences, something that depends on the location and orientation of the dipole source within the structure.
- Rather than simply evaluating the integrals in (2)–(5), we can plot the value of the integrand $I(u)$ as a function of the variable of integration, the normalized in-plane wavevector $u$. Such a plot gives us the power dissipation spectrum [15]. From such spectra, we may gain valuable insight into the nature of the modes that are present, and the strength with which the dipole is coupled to them.
- Additionally, we can compute the fractional power coupled to a specific mode by integrating the area under the power dissipation spectrum corresponding to that mode. Comparing this to the total area under the spectrum gives us the fractional power coupled to a specific mode [15], [20], [21], a technique referred to as selective integration.
- The model can be modified slightly to give the electric field outside the cavity region rather than at the dipole site. This then allows the Poynting vector to be computed. By integrating the Poynting vector over a particular plane, one can then find the power going through that plane [4], [22]. This is especially useful in calculating the power radiated by a given structure.

The power of this model can be put to immediate use by examining the modes of a typical polymer-based LED microcavity structure. The power dissipation spectrum and schematic of the structure to which it corresponds are shown in Fig. 3. The power dissipated in the interval $0 < u < 0.5$ may be radiated into the air [note that only a fraction (albeit often a very large one) of this power will ultimately be available as useful radiation since some will be reflected by the top glass/air interface and lost to absorption by cavity materials]. The power dissipated in the interval $0.5 < u < 0.73$ is trapped in the layers that make up the DBR mirror and the glass superstrate, that in the interval $0.73 < u < 1$ is confined to the DBR mirror. The large peak at $u = 1.02$ corresponds to dissipation of power to the surface plasmon polariton mode at the aluminum/polymer interface. This later feature is nonradiative, i.e., it has a wavevector greater than that of a photon of the same frequency in the polymeric material. However, the dipole source is able to couple directly to it since the near field of the dipole contains many high wavevector, evanescent components. This type of plot shows that a considerable fraction of the power dissipated by the dipole source does not produce useful radiation.

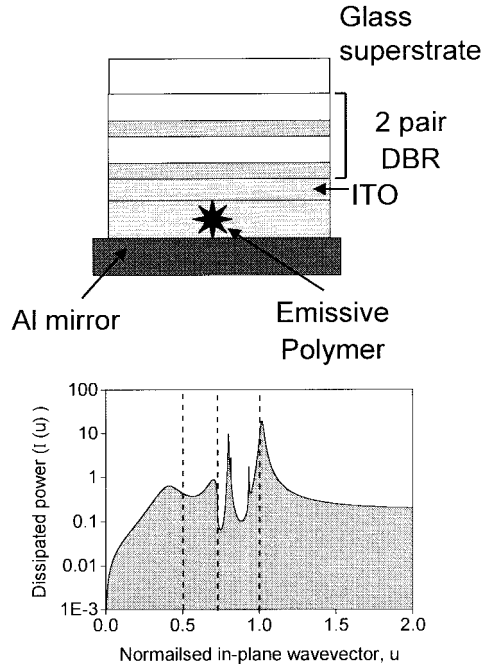


Fig. 3. A typical polymer microcavity LED structure and the associated calculated power dissipation spectrum for emission at 614 nm. The DBR comprises two high and low index pairs. The permittivity of the high (low) index layer is 5.13 (2.12) and has a thickness of 67.8 nm (105.4 nm). The polymer has a permittivity of 4.0 and a thickness of 118 nm, the emissive region being confined to a monolayer 10 nm from the aluminum mirror (which has a complex permittivity of $-70 + 30i$). The indium tin oxide electrode has a permittivity of 3.5 and a thickness of 40 nm. The medium above the DBR stack (a glass superstrate) has a permittivity of 2.12. The different regions of the power dissipation spectrum discussed in the text are delineated by vertical dashed lines. Note the logarithmic scale of the dissipated power. The emitters were assumed to behave according to the isotropic case (5).

$$I_{\perp}(u) = \frac{3}{2}\frac{u^3}{l_1}\frac{\left(1 - r^p_{1,2}e^{i\beta_{1,2}}\right)\left(1 - r^p_{1,3}e^{i\beta_{1,3}}\right)}{\left(1 - r^p_{1,2}r^p_{1,3}e^{i(\beta_{1,2}+\beta_{1,3})}\right)} \tag{3}$$

$$I_{\|}(u) = \frac{3}{4}\frac{u}{l_1}\left\{\frac{\left(1 + r^s_{1,2}e^{i\beta_{1,2}}\right)\left(1 + r^s_{1,3}e^{i\beta_{1,3}}\right)}{\left(1 - r^s_{1,2}r^s_{1,3}e^{i(\beta_{1,2}+\beta_{1,3})}\right)} + \left(1 - u^2\right)\frac{\left(1 + r^p_{1,2}e^{i\beta_{1,2}}\right)\left(1 + r^p_{1,3}e^{i\beta_{1,3}}\right)}{\left(1 - r^p_{1,2}r^p_{1,3}e^{i(\beta_{1,2}+\beta_{1,3})}\right)}\right\} \tag{4}$$

The concept of the proposed scheme for extracting this lost power from a thin emissive layer makes use of an intermediary guided mode, as outlined in Section II. This paper concerns the use of surface plasmon polaritons as the intermediary mode. The primary advantages of this mode over the more familiar dielectric waveguide type of guided mode are greater field enhancements, no lower frequency cutoff, and excellent confinement of the optical fields by the metal layer(s) used to support the SPP mode. These advantages and relevant background physics are discussed in the next section.

## VI. Surface Plasmon Polaritons

SPP's are a guided optical mode that may exist at the interface between a dielectric and a metal [23]. They consist of an oscillating electromagnetic field coupled to an oscillating surface charge density distribution, the latter being provided by the metal. The optical fields associated with such modes decay exponentially in strength with increasing distance from the interface that supports them. If we take Maxwells equations, apply the usual boundary (saltus) conditions for a planar interface, namely, that tangential $E$ and $H$ are continuous, and seek solutions that have the desired spatial dependence, we find that the dispersion relationship for the mode is given by

$$k_{\mathrm{spp}} = \frac{\omega}{c}\sqrt{\frac{\varepsilon_1\varepsilon_2}{\varepsilon_1+\varepsilon_2}} \tag{6}$$

where $\omega$ is the angular frequency and $\varepsilon_1$ and $\varepsilon_2$ are the relative permittivity of the dielectric and metal media, respectively.

These modes are in general nonradiative, i.e., $k_{\mathrm{spp}} > k_1$, where $k_1 = \sqrt{\varepsilon_1}k_0$, with $k_0 = \omega/c$, is the maximum wavevector that a photon (strictly a polariton) can have in the dielectric material in which the emitter is embedded. The surface charges in some sense "bind" the fields to the surface so that they cannot propagate away from the interface. This nonradiative character of SPP's has two important consequences for us.

- SPP modes cannot couple directly to photon-like modes (i.e., plane waves in the dielectric medium); their wavevector (momentum) is too great. If such coupling is desired, some kind of momentum change is required. Two common methods are prism coupling and Bragg scattering from a periodically modulated surface—usually that of the metal. The latter method is discussed in some detail below.
- The fields associated with the SPP mode are localized at the interface. As mentioned above, the near field of an oscillating dipole contains evanescent high wavevector components. If the distance between the dipole source and the metal/dielectric interface is on the order of the wavelength of the light involved, or less, direct coupling between the dipole source and SPP modes is possible.

Another consequence of the nonradiative character of SPP modes is that the fields associated with them may be considerably enhanced in strength when compared to those used to generate them. Thus, as the dipole source is brought closer to the metal/dielectric interface, the coupling to the SPP mode becomes stronger and the associated increase in decay rate may be substantial, which is examined below.

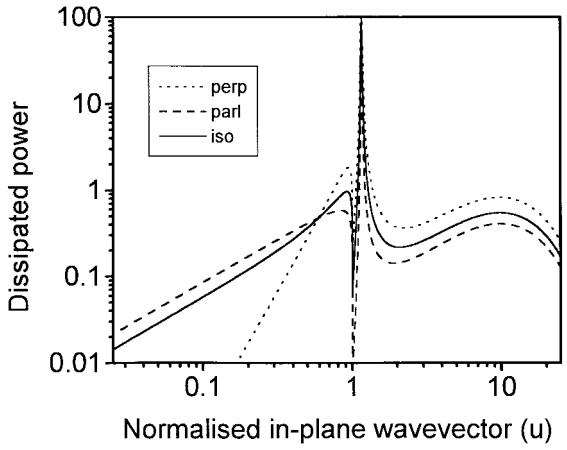


Fig. 4. The power dissipation spectrum of a dipole source embedded in a semi-infinite dielectric of permittivity $\varepsilon = 4$, located 5 nm from the interface between the dielectric and a semi-infinite silver medium (complex permittivity $-16 + 0.7i$ at the chosen wavelength of 633 nm). Data are shown for the three types of dipole orientation: perpendicular (dotted line), parallel (dashed line), and an isotropic mixture of the two (solid line). Note the logarithmic scale of the dissipated power.

A powerful way to examine this coupling is to use the power dissipation spectrum and selective integration techniques mentioned above. Fig. 4 shows the power dissipation spectrum for a dipole source embedded in a dielectric material, 5 nm from the interface between the dielectric and the noble metal silver. The fraction of power in the in-plane wavevector interval $0 \leq u \leq 1$ may give rise to radiation. This fraction of the emission corresponds to radiation although, as mentioned above, the radiation only emerges after it has "bounced round" in the structure (in this case simply reflected by the interface), during which some energy is lost by absorption to the microcavity materials. (For this reason the dissipated power in this interval is sometimes known as leaky.) The large contribution at $u = 1.14$ represents coupling to the SPP mode; the contribution in the interval $2 \leq u \leq \infty$ represents coupling of the oscillating dipole to electron scattering, excitation of electron hole pairs, etc. [24], a collection of processes that have been referred to as lossy surface waves [15].

Competition between coupling of the oscillating dipole to SPP modes and lossy surface waves is an important issue. The length scale associated with the two is different, approximately $\lambda$ for the SPP's and approximately $\lambda/100$ for the lossy surface waves. By selectively integrating the relevant sections of the power dissipation spectrum, the fraction of power dissipated via these routes may be evaluated (Fig. 5).

An optimum separation between source and interface exists that maximizes the coupling to the SPP mode (note that the details depend on the dipole orientation—Fig. 5). This competition with lossy surface waves is very important as it limits the enhancement that is available if SPP modes are to be used as a means by which light is to be extracted from the structure. For the data shown in Fig. 5, the greatest fraction of power coupled to the SPP mode is 98, 47, and 74% at a distance of 67, 16, and 20 nm from the metal interface, at

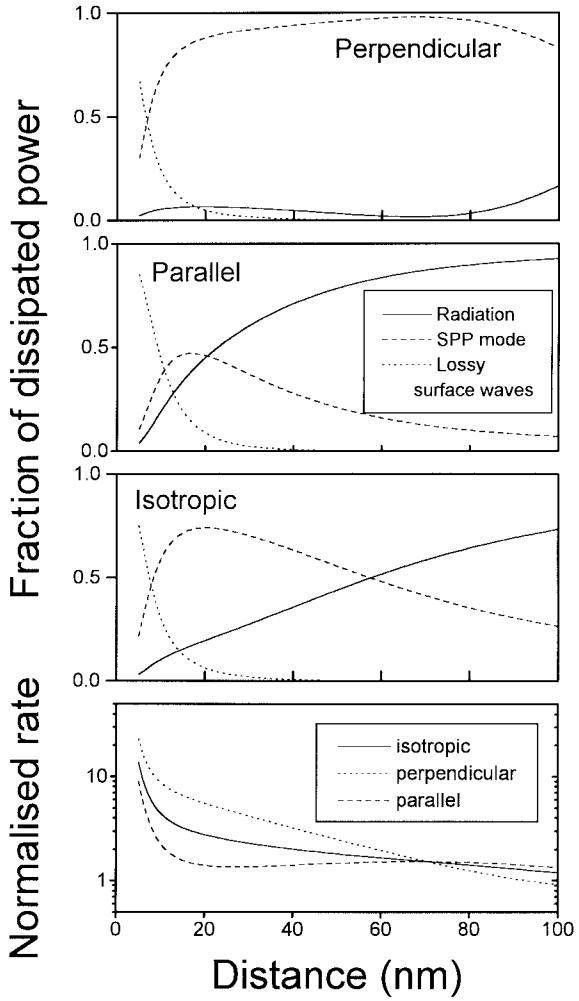


Fig. 5. The fraction of power going to different decay routes (modes) available to the emitter for the structure considered in Fig. 4—radiation (solid line), SPP mode (dashed line), and lossy surface waves (dotted line)—as a function of the distance between the emitter and the metal surface. The top three graphs are for the perpendicular, parallel, and isotropic dipole orientations. The lower graph shows the associated decay rate for the three orientations: isotropic (solid), perpendicular (dotted), and parallel (dashed).

which distance the normalized decay rate is 1.65, 1.5, and 2.8, respectively. (The three numbers refer to the three types of dipole orientation considered: perpendicular, parallel, and isotropic case, respectively.)

Using this type of model, it is also possible to build up a picture of the SPP mode by evaluating the power dissipation spectrum as a function of frequency. Fig. 6 shows such data where the contribution to the decay rate $I(u)$ is shown on a grayscale map as a function of both frequency and in-plane wavevector (note that the grayscale is a logarithmic one). The frequency dependence of $\varepsilon_2$, the dielectric permittivity of the metal, has been represented using the Drude model

$$\varepsilon_2(\omega) = 1 - \left( \frac{\omega_p^2}{\omega^2 + i\gamma\omega} \right) \tag{7}$$

where $\omega_p$ is the angular plasma frequency and $\gamma$ is the damping coefficient. For the silver films considered in this work, the values $\omega_p = 7.9$ eV and $\gamma = 0.06$ eV have been used.

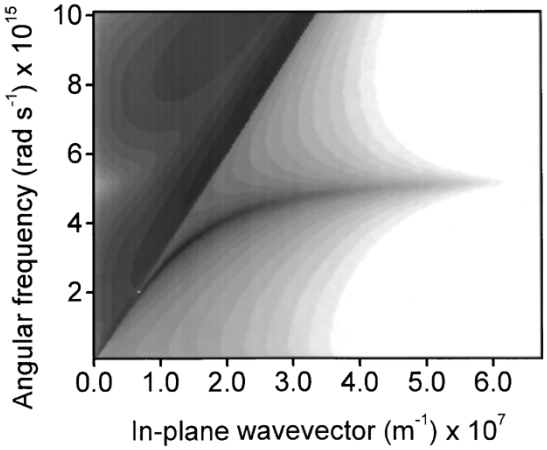


Fig. 6. The power dissipation spectrum shown as a function for both frequency and in-plane wavevector, exhibiting the dispersion of the SPP mode. The structure considered is the same as that of Fig. 4; the distance between the emitter and metal surface is 70 nm. The light line in the dielectric (representing the maximum in-wavevector a photon in the dielectric could have) is clearly seen as the straight edge feature. The dissipated power is plotted on a logarithmic grayscale, dark regions corresponding to a high level of power dissipation.

Fig. 6 shows an asymptotic limit above which the mode ceases to exist. This asymptotic limit is important since it means that the density of SPP modes at this frequency is very high *and* that very large values of in-plane wavevectors may couple to SPP modes at this frequency, This latter aspect is of particular interest in the context of extracting light from thin emissive layers. It indicates that structures with spatial dimensions in the range 10–100 nm may be used to support such modes. These structures may thus be significantly smaller than the dimensions associated with the standard $\lambda/2$ cavity typically considered for LED applications. If we can combine these dimensions with confinement of the optical field to within these dimensions, then the field strengths associated with these modes will be very high. If at the same time we can avoid significant coupling to lossy surface waves, we will have a good candidate system for our emission scheme.

While the asymptotic SPP frequency has some attractions as outlined above, it is not very flexible. In particular, the frequency cannot be tuned to match that of the emitter. Alternative ways of producing "flat bands" in the dispersion curve that also comprise high wavevectors are the subject of the next section.

## VII. Controlling SPP Modes

The SPP modes associated with a single metal/dielectric interface are really just the start. There are two types of more complex structure that have SPP modes associated with them that are of a more "tunable" character: the multilayer metallo-dielectric planar structure and the microstructured metal/dielectric interface.

### *A. Metallo-Dielectric Planar Multilayer Structures*

The fields associated with SPP modes decay exponentially with distance away from the metal/dielectric interface. If two such interfaces are close enough that the fields of mode each

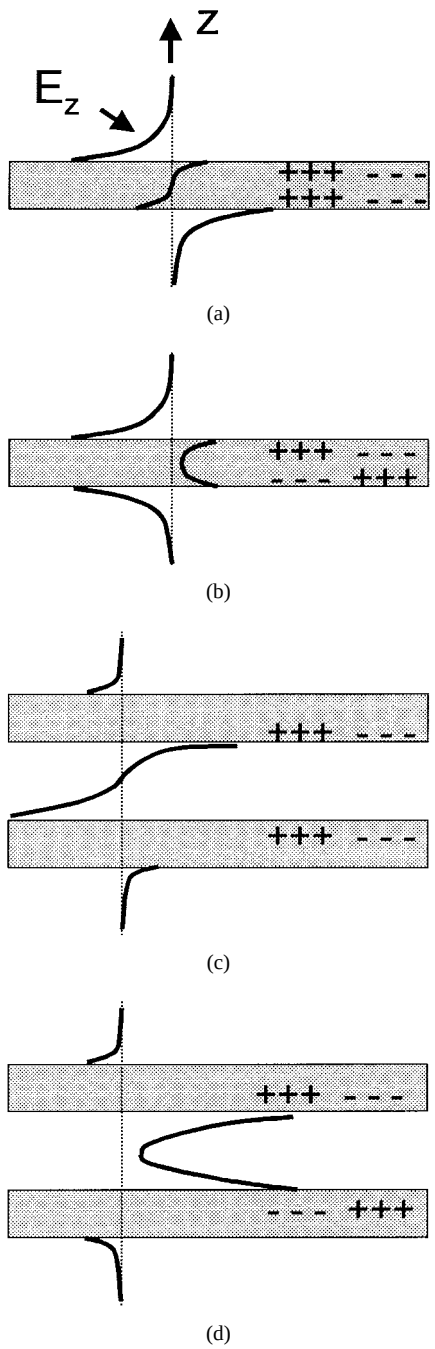


Fig. 7. The field profiles and associated surface charge density distributions of the coupled SPP modes. The field component drawn is the electric field normal to the cavity plane $E_z$. Schematics (a) and (b) are for the dielectric clad thin metal film, (a) being the symmetric mode (with respect to surface charge density) and (b) the asymmetric mode. Schematics of symmetric and asymmetric coupled SPP modes of (c) and (d) are for the metal clad dielectric cavity.

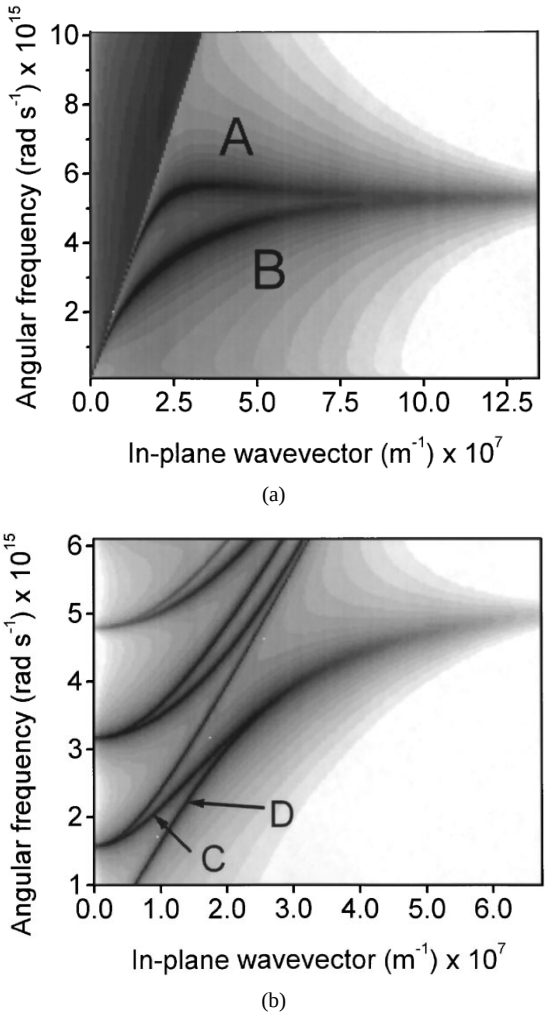


Fig. 8. Power dissipation spectra as a function of frequency and in-plane wavevector for the two coupled SPP mode structures: (a) is for the dielectric clad thin metal film and (b) is for the metal clad dielectric cavity. The grayscale is logarithmic, with dark regions indicating a high level of power dissipation.

overlap, and the modes of each interface have very similar values of in-plane wavevector, then the modes may interact. In fact, the eigenmodes of the new structure are not the simple SPP modes associated with each interface; rather, they are two coupled modes, each coupled mode being associated with both interfaces. There are two possible structures according to whether the medium between the interfaces is a metal or a dielectric. These are shown in Fig. 7 together with the associated field profiles and surface charge distributions of the different eigenmodes.

Fig. 8 shows the dispersion diagrams for the two cases as exhibited by the power dissipation spectrum of a dipole source close to a metal surface in each structure. For the dielectric clad thin metal film, Fig. 8(a), the field profiles of the two modes differ primarily in that one [labeled A in Fig. 8(a)] has a field zero in the intervening material, associated with the symmetric distribution of surface charge on the two interfaces [Fig. 7(a)]. The other solution, labeled B in Fig. 8(a), has an asymmetric charge distribution and a greater proportion of its field in the metal [Fig. 7(b)]. It therefore experiences greater loss and for this reason is sometimes known as the short-range coupled SPP, the other solution being known as the long-range coupled SPP [14]. Notice that the coupling of the two surfaces requires the dielectric permittivity seen by the modes on either side of the metal to be the same. Since the fields of the surface modes have limited spatial extent away from the interfaces, it is possible to achieve symmetry with the metal film bounded by media of differing permittivity. This may be done by coating the metal surface on the side

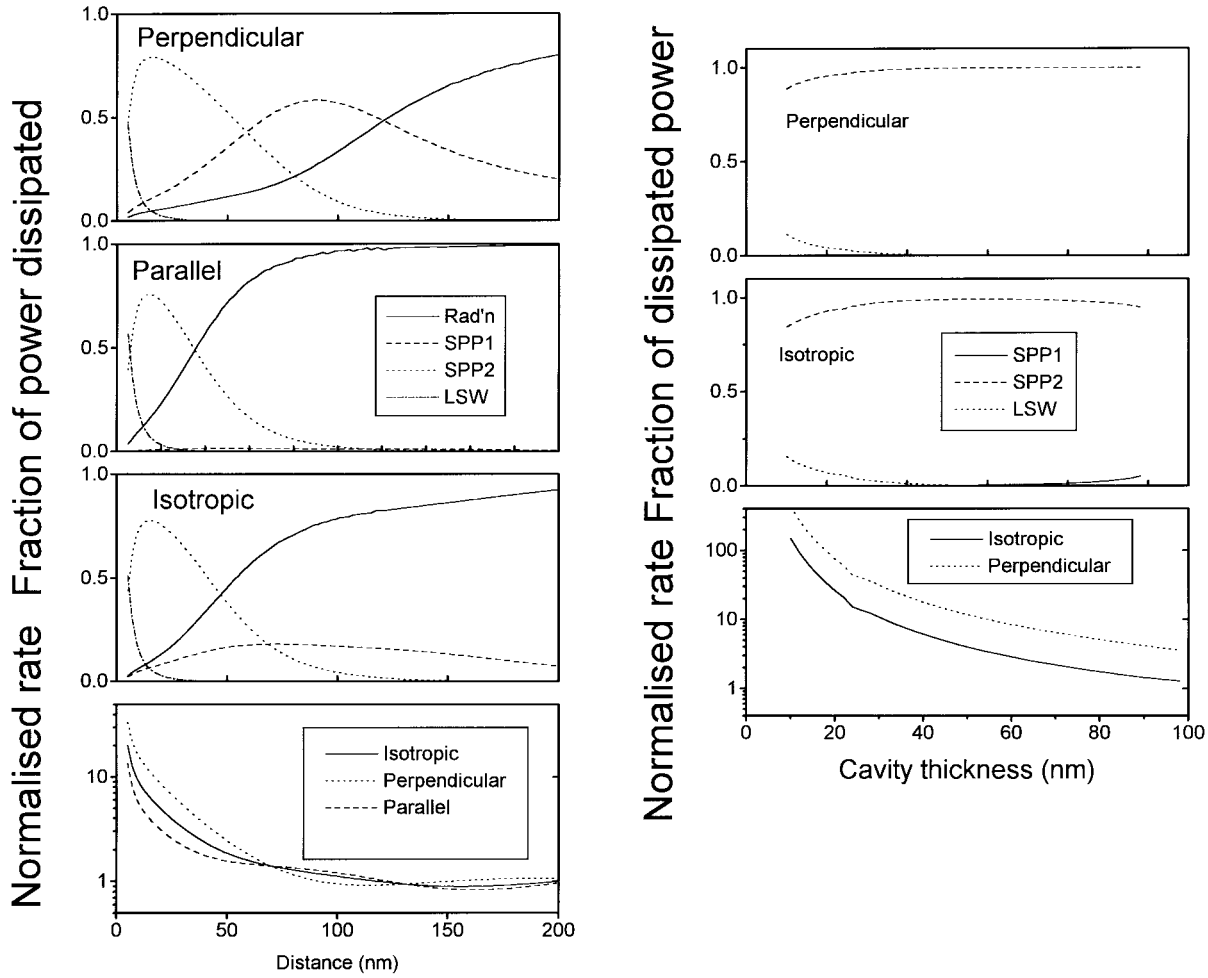


(a) (b)

Fig. 9. (a) The top three graphs show the calculated fraction of power dissipated via radiation (solid line), the symmetric coupled SPP mode (dashed line, SPP1), the asymmetric coupled SPP mode (dotted line, SPP2), and lossy surface waves (dash-dotted line) as a function of distance from one of the dielectric/metal interfaces of the dielectric clad thin metal film. The lower graph shows the associated decay rate. The structure is the same as that for Fig. 8(a). (b) The top three graphs show the calculated fraction of power dissipated to the symmetric coupled SPP mode (this mode is far below cutoff and so makes only a small contribution) (solid line, SPP1), the asymmetric coupled SPP mode (dashed line, SPP2), and lossy surface waves (dotted line) as a function of the thickness of the metal clad dielectric cavity. The source is maintained at the center of the cavity. The lower graph shows the associated decay rate. The structure is the same as that for Fig. 8(b).

bounded by the dielectric of low permittivity with a high-permittivity thin film of appropriate thickness. Coupling could also be achieved between the two modes of the interfaces of an asymmetrically clad system using Bragg scattering from periodic microstructure, an aspect discussed in Section VII-C.

For the metal clad dielectric cavity [Fig. 8(b)], the modes are similar in character, but the symmetry is different. The mode associated with curve $C$ of Fig. 8(b) is the symmetric mode (with respect to surface charges) of the metal clad cavity [Fig. 7(c)] and has a field zero at the center of the cavity. At low in plane wavevectors, the symmetric mode becomes the lowest order TM cavity mode. The other mode, labeled $D$ in Fig. 8(b), is the asymmetric mode and is degenerate with the first at high values of in-plane wavevector. The dispersion of this mode is similar to that of the single interface mode, Fig. 6 [25]. Fig. 8(b) shows another fascinating feature for mode $D$: it is a cavity mode that has no cutoff. The dimensions of the cavity can thus be reduced below the usual cutoff and the mode will be better confined, the large negative real component of the metal's permittivity enabling this confinement. As a consequence of this greater confinement, the strength of the fields associated with the mode also rise, providing greater potential for increasing the spontaneous emission rate.

Of particular importance to us here is the extent to which our dipole source may couple to the SPP mode [26], i.e., what is the greatest fraction of power that may be coupled to the relevant SPP mode? When this occurs, what change in the rate is associated with it? We can get an indication by selectively integrating the power dissipation spectrum as described above; the results are shown in Fig. 9.

From the data displayed in Fig. 9(b), we see that the metal clad microcavity offers the best opportunity. At a cavity thickness appropriate to couple 90% of the power to the asymmetric SPP mode (the dominant mode), the normalized decay rate for the isotropic and perpendicular cases is 45 and 330, respectively. The parallel aligned dipole is unable to couple to the symmetric coupled SPP mode when placed at the center of the cavity. Further calculations (not shown)

indicate that offsetting the position of the emitter from the cavity center allows coupling for the parallel aligned dipole, but it is very weak compared to the perpendicular orientation. Further, this small benefit in coupling between the emitter and the SPP mode is at the expense of increased dissipation to lossy surface waves. Although more work is required, it looks as though the middle of the cavity is the optimum position for the isotropic case. The high enhancement of the rate and high fraction of power coupled to the symmetric coupled SPP mode of the metal clad microcavity can be obtained with the dipole source still far enough from metal to avoid significant coupling to the lossy surface waves.

The same is not true for the thin metal film structure. Here again, the asymmetric coupled SPP mode is the dominant one. For the perpendicular, parallel, and isotropic cases, the maximum fraction of power coupled to the asymmetric SPP mode is 79, 75, and 77% at distances of 17, 14, and 15 nm for which the associated normalized decay rates are 10, 4, and 6, respectively.

Of course, coupling between the dipole source and the SPP mode is just half of the process; there remains the important business of coupling the SPP out to useful radiation, a topic we discuss below. The proposal here is to use periodic microstructure to obtain the required coupling, although prism coupling is also a possibility [14]. However, microstructure may also be used to further modify the dispersion of the SPP modes, which we examine next.

### *B. Periodic Microstructure and SPP Mode Dispersion*

Changes to the dispersion of SPP modes more dramatic than those mentioned above occur when one moves away from the restriction of a planar interface. We start by considering a surface that possesses a simple sinusoidal corrugation on the scale of the wavelength of light—a metallic diffraction grating. The simplest effect of such a surface is to allow the SPP mode to Bragg scatter from the periodic modulation, so reducing (or increasing) the in-plane wavevector. When scattering reduces the wavevector, the mode may couple to radiation. This phenomenon has been observed many times, particularly in the production of radiation by fluorescing species in close proximity to a surface that can be considered a metallic diffraction grating [11].

If the pitch of the corrugation is sufficiently short, coupling of the SPP to radiation may no longer be possible since $k_{\rm spp} - k_g < k_1$. If, however, $k_{\rm spp} - k_g = -k_{\rm spp}$, then the corrugation is such that a forward traveling SPP mode is scattered into a backward traveling SPP mode. The two counter-propagating modes set up a standing wave that has two eigensolutions. One solution has field extrema at the peaks of the corrugation and is labeled $\omega_-$. The other solution has field extrema at the grating troughs and is labeled $\omega_+$. These two solutions have different energies associated with them owing to their different field and surface charge distributions. However, the high-energy ($\omega_+$) and low-energy ($\omega_-$) solutions both have the same wavevector, dictated by the periodicity of the corrugation. A bandgap is thus opened up [27]. In this way, our simple surface electromagnetic crystal, a metallic diffraction grating, produces bandgaps in much the same way as "bulk" dielectric electromagnetic crystals produce bandgaps for photon-like modes. A schematic of the dispersion curve of such a surface is shown in Fig. 10.

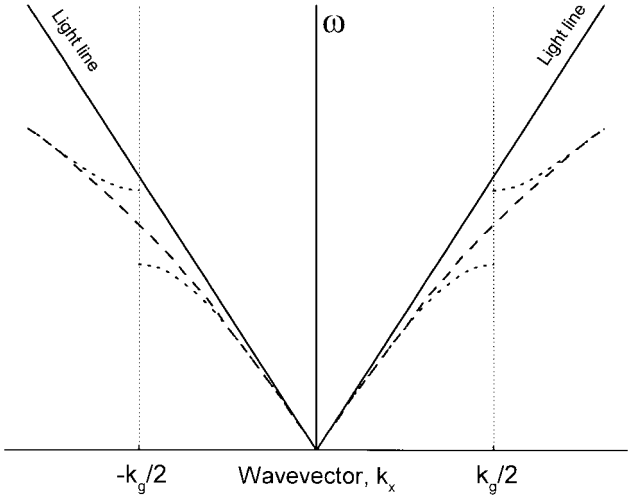


Fig. 10. The surface plasmon polariton dispersion curve in terms of the angular frequency $\omega$ and the in-plane wavevector $k_x$. The dashed line is the dispersion curve for a flat surface, and the dotted line for a corrugated surface. A frequency gap is opened up in the corrugated case. The gap occurs at $\pm k_g/2$, the Bragg vector of the corrugation being $k_g$. Also shown are the light lines. These are the dispersion curves for photons traveling at grazing incidence to the interface between the metal and the dielectric, i.e., those having the largest possible value of $k_x$, the in-plane wavevector.

Three things should be noted here.

1) The modes at the band edges are stationary (their group velocity is zero).
2) The mode density at the band edges is high—something we are trying to achieve, as outlined above, since it leads to the possibility for significant enhancement of the SPP decay route.
3) The position (frequency) of these band edges, and the degree of band flattening associated with them, is dictated by the profile of the periodic surface, and may thus be controlled.

In fact, we have cheated somewhat here since we have only considered SPP modes propagating in one direction along the surface, parallel to the Bragg vector associated with the corrugation [28]. A bandgap that prohibits propagation in all directions on the surface may be made by introducing further periodic corrugations (in different directions) to the surface profile [29]. Periodic corrugations have also been used to block the asymmetric metal clad microcavity mode [30].

A radical change to the dispersion curve of Fig. 10 can be made by making the troughs of the corrugation considerably deeper [31]. In this case, the nature of the surface changes to the extent that we have a situation not so dissimilar from the metal clad microcavity, i.e., in the trough, we have two roughly parallel metal surfaces separated by a dielectric. Our SPP mode exists on both surfaces and is thus able to interact with itself to produce a coupled, resonant mode. The big difference between this and the metal clad microcavity mentioned above is the limited spatial extent of the cavity in the present case. The resonant coupled mode has a field loop associated with the trough. Increasing the frequency (or increasing the depth of

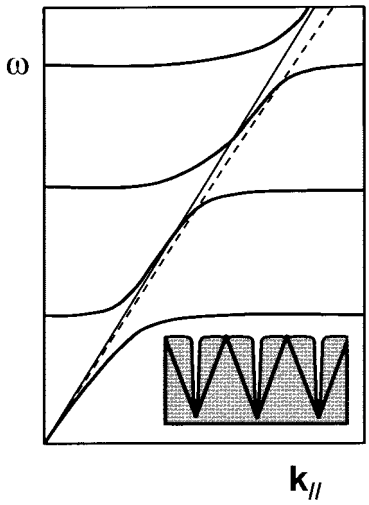


Fig. 11. Schematic of the dispersion curve for the deep grating structure shown in the inset. The dashed line is the dispersion of the SPP mode in the absence of the grooves.

the groove) will allow the introduction of a second resonant mode possessing two field loops in the trough, and so on.

The technique we have used so far to examine the dispersion of SPP modes, that of mapping the power dissipation spectrum of an oscillating dipole embedded within the structure, has not yet been implemented to calculate similar properties of nonplanar structures, although a start has been made [32], [33]. However, the dispersion curve may be studied by examining the scattering matrix of the structure for incident plane waves of arbitrary wave vector. A numerical procedure for doing this has recently been developed [31], and the results for a surface possessing deep corrugated grooves are shown as a schematic in Fig. 11.

Electric field enhancements of order 50 have been predicted [34]. This type of structure has also been examined for its role in the SERS effect, where very large field enhancements have been calculated in the base of troughs that have the form of a cusp [35], [36].

While showing that periodically modulated surfaces offer significant field enhancements through their ability to support coupled SPP modes, they do not appear to provide a practical route by which emission from a thin emissive film may be extracted: sources would have to be located within the troughs. A more practical approach may be to work with a metal film that is optically thin, rather than a semi-infinite one (i.e., optically thick); we want the coupled SPP mode to act as an aerial for our small oscillating dipole sources. What may be needed is to place our sources on one side of a periodically modulated metal film, close enough to it so that they couple effectively to the SPP modes, far enough away from it to avoid coupling to lossy surface waves. The SPP modes need then to be efficiently coupled to radiation, an aspect we will consider later.

Let us accept for the moment the need for the sources to be on one side of the metal film, ultimately to produce radiation on the far side of the metal via an intermediate step, an SPP mode. We appear to be faced with at least four possibilities.

1) We could use a thin metal film, asymmetrically clad, but possessing periodic microstructure that couples the modes of the two surfaces together. We mentioned in Section VII-A that this did not provide as big a potential enhancement as the metal clad microcavity, but it does have the advantage of simplicity.
2) We may use the coupled SPP modes of the planar metal clad microcavity mentioned in Section VII-A. Coupling to radiation in this case takes place across the metal film.
3) We may extend the approach described above of using deep troughs so as to produce a periodic array of holes in a thin metal film. In this case, we anticipate that coupled modes will exist in the holes, resonant when the length of the hole (thickness of the metal film) is such that it forms a resonant cavity via reflections at the "ends" of the hole. Coupling to radiation in this case takes place through the holes.
4) We could adopt a slight variant of the approach just mentioned. Instead of using an array of holes, we could make use of a periodic array of metallic particles. Such metallic particles have resonances associated with them that occur when the size of the particle is such that the SPP mode is in phase with itself, having propagated around the particle. Such structures are common to the SERS effect and well known for the local field enhancements they produce. The resonances are the equivalent of the Mie resonances of a dielectric particle. Coupling to radiation in this case takes place "around" the metallic particles.

Which of these four approaches is best? More fundamentally, will any of them be efficient enough in coupling power from our emissive species to radiation to provide a real advantage over other techniques? If an increase in the spontaneous emission rate is also important, what is the best compromise between rate and efficiency?

To summarize, the two stages involved with each structure are coupling of the dipole emission to the appropriate SPP mode, followed by coupling of the SPP mode to useful radiation. Of critical importance is the issue of avoiding dissipation of power in the metal. Such dissipation will occur while the energy is in the form of the SPP mode since it is this mode that has fields that may significantly penetrate the metal. We thus require that coupling of the SPP to radiation occur at a higher rate than that at which the SPP mode dissipates its energy in the metal. It might be thought that this problem of dissipation in the metal precludes the viability of the proposed scheme. However, the propagation length of a single planar interface SPP mode is of order $>20\ \lambda$ [23]. Where periodic microstructure is used to couple the SPP mode to radiation (e.g., the diffraction grating), the periodicity is typically of order $\lambda$. Provided that less than about 20 "bumps" are needed to ensure efficient coupling to radiation, radiation will be more effective (have a higher rate) than dissipation. The efficiency of this process has been measured to be $>80\%$ [37]. Additional optimism can be gained from noting that the large enhancements for the SERS effect *are* seen [38]. Let us now turn to examining the four schemes under consideration in turn.

### C. The Thin Metal Film

Here the emitters are embedded just below the surface of a dielectric material, and a metal film is deposited on

top, together with suitable microstructure. The emitters are coupled primarily to the asymmetric mode of this structure. As mentioned above, this scheme has the disadvantage of a relatively low potential enhancement when compared to the metal clad cavity, but is attractive due to its simplicity. The viability of the scheme has already been demonstrated in experiments where molecular fluorescence was converted into radiation on the far side of the metal film, microstructure being used to both couple the SPP modes together and scatter the top surface SPP mode to provide radiation [39].

As with all the schemes discussed here, we have been considering only one-dimensional periodic microstructure so far for use in coupling SPP modes to radiation. As with the use of microstructure to generate bandgaps, discussed in Section VII-B, microstructure periodic in two dimensions will be required to couple as much as possible of the energy to useful radiation [32].

### *D. The Metal Clad Microcavity*

In this case, the emitters reside within the microcavity, thus allowing them to couple efficiently to the asymmetric coupled SPP mode of this structure. To couple this SPP mode to radiation, the planar structure needs to be modified so that it possesses the required periodicity. To couple this mode to normally emitted radiation, the periodicity of the microstructure $k_g$ must be such that $k_g \sim k_{\rm spp}$. Note that emission in the backward direction is blocked by the use of an optically thick lower metallic layer. How efficiently may our imposed microstructure couple the SPP mode to radiation? As mentioned above, we have no way at present of calculating this. However, we may gain some idea by looking at how efficiently light impinging from outside may couple into this SPP mode via scattering off the microstructure [40].

Numerical calculations based on a coordinate transformation technique [41] show that as expected, the degree of coupling depends on the depth of the grooves, as shown in Fig. 12, and that the coupling can be efficient: more than 90% of the power may be coupled to the SPP mode. While we cannot directly take this result to imply that the reverse process will be as efficient, it does provide encouragement.

### *E. Coupled SPP Modes of Holes in Metals—The Periodic Hole Array*

In this case, our thin metal film with its array of holes lies close to the emissive layer. Several issues are immediately apparent. The hole only occupies a relatively limited fraction of the surface of the metal film. How then may emitters located in a region not immediately adjacent to a hole, i.e., between holes, couple to the SPP modes of the holes? One might expect that the SPP modes associated with the holes will "spill over" at the apertures. Indeed, this may have already been observed in the experiments reported by the NEC group [42], [43]. They measured a transmission of ~10%, while the holes represent only 5% of the area, and standard diffraction theory predicts a transmission of 0.1%. The mechanism by which this transmission is achieved, in particular the role played by the resonant SPP modes of the holes, is still not clear. While

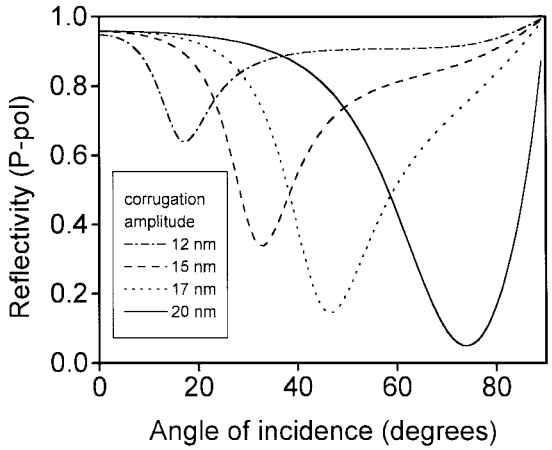


Fig. 12. The calculated P-polarized reflectivity of a metal clad cavity. The top metal mirror is 20 nm thick and the cavity 25 nm thick; the lower mirror is semi-infinite in extent. A wavelength of 612 nm was used, the permittivity of the metal being taken as $\varepsilon = 16.0 + 0.7i$, while the permittivity of the cavity medium was $\varepsilon = 4.0$. All of the interfaces have been given a periodic modulation so that each interface has an identical sinusoidal profile. The corrugation pitch was 140 nm, and the data are shown for several corrugation amplitudes, indicated in the inset box of the figure.

further work is needed to elucidate this mechanism, we note a potential problem associated with such a structure for our purposes.

To make use of the high fields of the SPP modes associated with the holes, the emitters need to be placed close to the metal/dielectric interface. Can they be placed close enough to achieve a significant effect while still only suffering minimal decay to lossy surface waves? Until we know more about the modes associated with the periodic hole array, these questions cannot be adequately answered.

What aspect of the microstructure is needed to couple the SPP modes to radiation? How efficiently does the mode radiate due to scattering off the end of the hole? Is further scattering off some other aspect of the structure required? Clearly, a lot of work is required in this area before the potential of the scheme can be properly assessed. The situation is not much clearer for the case of metal particles rather than holes.

### *F. Periodic Array of Metal Particles*

The resonant SPP modes associated with metallic particles have been known for some time [44]. The optical properties of these particles are well accounted for by the classical electromagnetic formalism of Mie scattering. As with the holes described in the previous section, changing the particle size and/or shape allows control over the resonant frequencies. It may be that rather than solid metal particles, ones comprising a shell of metal surrounding a dielectric are more useful. It appears that such structures afford greater control over the resonant frequencies through changes in particle size [45].

Many of the questions raised about the periodic array of holes have a counterpart here. Can all emitters within a thin layer achieve effective access to the SPP modes of the particles? Or are there regions where coupling is poor in between the particles? Does coupling to the resonant SPP modes compete effectively with dissipation to the lossy surface

waves? Likewise, questions concerning the coupling of the SPP modes to useful radiation need to be addressed. Does an individual particle radiate effectively? Is scattering off a periodic structure, i.e., periodic array of particles, of benefit? For both this and the previous hole array structure, how is downward-going radiation to be prevented?

## VIII. Summary

We have reached a point where there are far more questions than answers. The intention of this paper has been to highlight both the possible opportunities and potential problems associated with using SPP modes to extract power from thin films of emissive materials. Some suggestions have been made but, in that we are at an early stage in this area, it is quite possible that some different scheme will eventually emerge. Limitations on the potential performance calculated here do not take account of such technical problems as surface roughness; they will need to be investigated. Whether or not any of these approaches will develop into practical applications is even less clear. It is hoped that the present discussion will help to stimulate new research into this fascinating area. Whatever the outcome, we will at least learn a lot about the SPP modes of various periodic structures and the physics of surface electromagnetic crystals.

## Acknowledgment

The author wishes to thank J. R. Sambles, P. Andrew, P. T. Worthing, M. G. Salt, J. A. Wasey, I. D. W. Samuel, and T. F. Krauss, among others.

## References

[1] *Digest of United Kingdom Energy Statistics*. London, U.K.: Government Statistical Service (ISBN 011 5154477), 1997.
[2] N. C. Greenham, R. H. Friend, and D. D. C. Bradley, "Angular dependence of the emission from a conjugated polymer light emitting diode: Implications for efficiency calculations," *Adv. Mater.*, vol. 6, no. 6, pp. 491–494, 1994.
[3] H. Benisty, H. De Neve, and C. Weisbuch, "Impact of microcavity effects on light extraction—Part 2: Selected exact simulations and role of photon recycling," *IEEE J. Quantum Electron.*, vol. 34, pp. 1632–1643, Sept. 1998.
[4] J. A. E. Wasey and W. L. Barnes, submitted for publication.
[5] R. E. Slusher and C. Weisbuch, "Optical microcavities in condensed matter systems," *Solid State Commun.*, vol. 92, no. 1/2, pp. 149–158, 1994.
[6] A. Dodabalapur, L. J. Rothberg, R. H. Jordan, T. M. Miller, R. E. Slusher, and J. M. Phillips, "Physics and applications of organic microcavity light emitting diodes," *J. Appl. Phys.*, vol. 80, no. 12, pp. 6954–6964, 1996.
[7] R. H. Friend, R. W. Gymer, A. B. Holmes, J. H. Burroughs, R. N. Marks, C. Taliani, D. D. C. Bradley, D. A. Dos Santos, J. L. Brédas, M. Lögdlund, and W. R. Salaneck, "Electroluminescence in conjugated polymers," *Nature*, vol. 397, no. 6175, pp. 121–128, Jan. 15, 1999.
[8] S. D. Brorson, H. Yokoyama, and E. P. Ippen, "Spontaneous emission rate alteration in optical waveguide structures," *IEEE J. Quantum Electron.*, vol. 26, pp. 1492–1499, Sept. 1990.
[9] T. Baba, R. Watanabe, K. Asano, F. Koyama, and K. Iga, "Theoretical and experimental estimations of photon recycling effect in light emitting devices with a metal mirror," *Jpn. J. Appl. Phys.*, vol. 35, pt. 1, no. 1A, pp. 97–100, Jan. 1996.
[10] R. Windisch, P. Heremans, A. Knobloch, P. Kiesel, G. H. Döler, B. Dutta, and G. Borghs, "Light emitting diodes with 31% external quantum efficiency by outcoupling of lateral waveguide modes," *Appl. Phys. Lett.*, to be published.
[11] S. C. Kitson, W. L. Barnes, and J. R. Sambles, "Photoluminescence from dye molecules on silver gratings," *Opt. Commun.*, vol. 122, pp. 147–154, 1995.
[12] B. J. Matterson, M. G. Salt, W. L. Barnes, and I. D. W. Samuel, "Effect of lateral microstructure on conjugated polymer luminescence," *Adv. Mater. Process.*, to be published.
[13] A. M. Vrendenberg, N. E. J. Hunt, E. F. Schubert, D. C. Jacobson, J. M. Poate, and G. J. Zydzik, "Controlled spontaneous emission from $Er^{3+}$ in a transparent $Si/SiO_2$ microcavity," *Phys. Rev. Lett.*, vol. 21, no. 4, pp. 517–520, July 26, 1993.
[14] Z. Lenac and M. S. Tomaš, "Enhanced molecular fluorescence mediated by long-range surface polaritons," *Surf. Sci.*, vol. 215, pp. 299–318, 1989.
[15] G. W. Ford and W. H. Weber, "Electromagnetic interactions of molecules with metal surfaces," *Phys. Rep.*, vol. 113, no. 4, pp. 195–287, 1984.
[16] G. Björk, S. Machida, Y. Yamamoto, and K. Igeta, "Modification of spontaneous emission rate in planar dielectric microcavity structures," *Phys. Rev. A*, vol. 44, no. 1, pp. 669–681, July 1, 1991.
[17] W. L. Barnes, "Fluorescence near interfaces: The role of photonic mode density," *J. Mod. Opt.*, vol. 45, no. 4, pp. 661–699, 1998.
[18] M. Born and E. Wolf, *Principles of Optics.* New York: Pergamon, 1975.
[19] J. E. Sipe, "The dipole antenna problem—I: Surface physics: A new approach," *Surf. Sci.*, vol. 105, pp. 489–504, 1981.
[20] P. T. Worthing, R. M. Amos, and W. L. Barnes, "Modification of the spontaneous emission rate of $Eu^{3+}$ ions embedded within a dielectric layer above a silver mirror," *Phys. Rev. A*, vol. 59, no. 1, pp. 865–872, 1999.
[21] H. Rigneault and S. Monneret, "Modal analysis of spontaneous emission in a planar microcavity," *Phys. Rev. A*, vol. 54, no. 3, pp. 2356–2368, 1996.
[22] L. Novotny, "Allowed and forbidden light in near–field optics—A single dipolar light source," *J. Opt. Soc. Am. A*, vol. 14, no. 1, pp. 91–104, Jan. 1997.
[23] H. Raether, *Surface Plasmons.* Berlin, Germany: Springer, 1988.
[24] P. Avouris and B. N. J. Persson, "Excited states at metal surfaces and their nonradiative relaxation," *J. Phys. Chem.*, vol. 88, pp. 837–848, 1984.
[25] K. R. Welford and J. R. Sambles, "Coupled surface plasmons in a symmetric system," *J. Mod. Opt.*, vol. 35, no. 9, pp. 1467–1483, 1988.
[26] P. T. Worthing and W. L. Barnes, "Spontaneous emission within metal clad microcavities," *J. Opt. A: Pure App. Opt.*, vol. 1, pp. 501–506, 1999.
[27] W. L. Barnes, T. W. Preist, S. C. Kitson, and J. R. Sambles, "Physical origin of photonic energy gaps in the propagation of surface plasmons on gratings," *Phys. Rev. A*, vol. 54, no. 9, pp. 6227–6244, 1996.
[28] W. L. Barnes, S. C. Kitson, T. W. Preist, and J. R. Sambles, "Photonics surfaces for surface-plasmon polaritons," *J. Opt. Soc. Am. A*, vol. 14, no. 7, pp. 1654–1661, July 1997.
[29] S. C. Kitson, W. L. Barnes, and J. R. Sambles, "Full photonic band gap for surface modes in the visible," *Phys. Rev. Lett.*, vol. 77, no. 13, pp. 2670–2673, Sept. 23, 1996.
[30] ——, "Photonic band gaps in metallic microcavities," *J. Appl. Phys.*, vol. 84, no. 5, pp. 2399–2403, Sept. 1998.
[31] W.-C. Tan, T. W. Preist, J. R. Sambles, and N. P. Wanstall, "Surface plasmon polariton bands on short pitch metal gratings," *Phys. Rev. B*, vol. 59, no. 19, pp. 12,661–12,666, May 15, 1999.
[32] H. Rigneault, F. Lemarchand, A. Sentenac, and H. Giovanini, "Extraction of light from sources located inside waveguide grating structures," *Opt. Lett.*, vol. 24, no. 3, pp. 148–150, 1999.
[33] C. Amra and S. Maure, "Electromagnetic power provided by sources within multilayer optics: Free-space and modal patterns," *J. Opt. Soc. Amer.*, vol. 14, no. 11, pp. 3102–3113, 1997.
[34] W.-C. Tan, private communication.
[35] F. J. García-Vidal and J. B. Pendry, "Collective theory of surface enhanced Raman scattering," *Phys. Rev. Lett.*, vol. 77, no. 6, pp. 1163–1166, Aug. 5, 1996.
[36] T. López-Rios, D. Mendoza, F. J. García-Vidal, J. Sánchez-Dehesa, and B. Pannetier, "Surface shape resonances in lamellar metallic gratings," *Phys. Rev. Lett.*, vol. 81, no. 3, pp. 665–668, July 20, 1998.
[37] J. Moreland, A. Adams, and P. K. Hansma, "Efficiency of light emission from surface plasmons," *Phys. Rev. B*, vol. 25, no. 4, pp. 2297–2300, Feb. 15, 1982.
[38] A. Otto, I. Mrozek, H. Grabhorn, and W. Akemann, "Surface enhanced Raman scattering," *J. Phys. Condens. Mat.*, vol. 4, pp. 1143–1212, 1992.
[39] R. W. Gruhlke, W. R. Holland, and D. G. Hall, "Surface plasmon cross coupling in molecular fluorescence near a corrugated thin metal film," *Phys. Rev. Lett.*, vol. 56, no. 26, pp. 2838–2841, June 30, 1986.

[40] W. L. Barnes and P. T. Worthing, "Spontaneous emission and metal clad microcavities," *Opt. Commun.*, to be published.
[41] N. P. K. Cotter, T. W. Preist, and J. R. Sambles, "A scattering matrix approach to multilayer diffraction," *J. Opt. Soc. Amer. A*, vol. 12, pp. 1097–1103, 1995.
[42] T. W. Ebbersen, H. J. Lezec, H. F. Ghaemi, T. Thio, and P. A. Wolff, "Extraordinary optical transmission through sub-wavelength hole arrays," *Nature*, vol. 391, pp. 667–669, 1998.
[43] H. F. Ghaemi, T. Thio, D. E. Grupp, T. W. Ebbesen, and H. J. Lezec, "Surface plasmons enhance optical transmission through subwavelength holes," *Phys. Rev. B*, vol. 58, no. 11, pp. 6779–6782, Sept. 15, 1998.
[44] T. Klar, M. Perner, S. Grosse, G. von Plessen, W. Spirkl, and J. Feldmann, "Surface plasmon resonances in single metallic nanoparticles," *Phys. Rev. Lett.*, vol. 80, no. 19, pp. 4249–4252, May 11, 1998, and references therein.
[45] S. J. Oldenburg, R. D. Averitt, S. L. Westcott, and N. J. Halas, "Nanoengineering of optical resonances," *Chem. Phys. Lett.*, vol. 288, pp. 243–247, May 22, 1998.

**W. L. Barnes**, photograph and biography not available at the time of publication.